Dynamic-to-static crossover in the acoustic attenuation of v-GeO_2

2007 EPL 78 36001

(http://iopscience.iop.org/0295-5075/78/3/36001)

A Letters Journal Exploring the Frontiers of Physics

May 2007

EPL, **78** (2007) 36001 www.epljournal.org
doi: 10.1209/0295-5075/78/36001

Dynamic-to-static crossover in the acoustic attenuation of v-GeO_2

G. Baldi[1,7], P. Benassi[2,7], L. E. Bove[3,7], S. Caponi[1,7], E. Fabiani[4], D. Fioretto[5,7], A. Fontana[1,7], A. Giugni[2,7], M. Nardone[2,7], M. Sampoli[6,7] and F. Scarponi[5]

[1] *Dipartimento di Fisica, Università di Trento - 38050 Povo, Trento, Italy*
[2] *Dipartimento di Fisica, Università di L'Aquila - 67010 Coppito, L'Aquila, Italy*
[3] *Departement Physique des Milieux Denses CNRS-IMPMC, Universitè Paris 6 - F-75015 Paris, France*
[4] *Universitè Joseph Fourier c/o Institut de Biologie Structurale and CRG-IN13 at Institut Laue-Langevin (ILL) - B.P. 156 Grenoble Cedex 9, France*
[5] *Dipartimento di Fisica, Università di Perugia - 06123 Perugia, Italy*
[6] *Dipartimento di Energetica, Università di Firenze - 50139 Firenze, Italy*
[7] *Research Center SOFT INFM-CNR, c/o Università di Roma "La Sapienza" - 00185 Roma, Italy*

received 11 September 2006; accepted in final form 15 March 2007
published online 16 April 2007

PACS 63.50.+x – Vibrational states in disordered systems
PACS 78.35.+c – Brillouin and Rayleigh scattering; other light scattering
PACS 61.12.Ex – Neutron scattering (including small-angle scattering)

Abstract – The acoustic attenuation of vitreous germania (v-GeO_2) has been measured over more than three decades in frequency, by means of neutron scattering at high-frequency (THz), visible light scattering and the newly developed technique of Brillouin ultraviolet scattering at lower frequencies (15–50 GHz). The experiments are supported by a molecular dynamics study of a simulated sample of v-GeO_2. The temperature dependence, from 80 K up to the glass transition temperature, shows a persistence of the dynamical nature of the attenuation in the GHz range and a simultaneous increase of the contribution coming from the structural disorder. At higher frequencies clear evidences of a crossover to a region where the attenuation is induced only by the topological disorder are found.

Introduction. – The way an acoustic excitation propagates in a topologically disordered solid remains one of the less understood subjects in the theory of amorphous materials [1]. A complete description of all the mechanisms responsible for sound attenuation is still lacking, despite great efforts both from experiments [2–6] and theory [7,8], mainly because the frequency range lying between the one accessed by ultrasonic absorption (US) and Brillouin light scattering (BLS) [3,4] and the one accessed by inelastic Brillouin neutrons (BNS) and X-rays scattering (IXS) [6] has remained until now unexplored. In US and in BLS experiments [2] the dynamics of glasses is probed on a length scale much greater than the interatomic distance. In this regime the amorphous solids, even the highly porous systems [9], behave like an elastic isotropic medium and the sound attenuation is found to be strongly temperature dependent showing, almost universally, a broad maximum below the glass transition temperature. With increasing frequency, the position of the maximum increases smoothly and its amplitude increases almost linearly in a wide frequency window [2,10]. Such a behavior is generally explained in terms of a thermally activated relaxation process with the relaxation time following an Arrhenius-type activation law. On the contrary, in BNS and IXS experiments which probe a length scale comparable to the interparticle distance, typical strong glasses [11], like v-SiO_2, v-GeO_2 and v-B_2O_3, show a short-range order quite similar to their crystalline counterpart [12]. The frequencies corresponding to these short distances lie in the THz range where the attenuation is found to be essentially temperature independent and to scale approximately with the square of the frequency (or of the exchanged wave vector q) [6]. The investigation of the glassy dynamics in the intermediate frequency range, from tens of GHz, the region covered by BLS, up to one THz (IXS and BNS), has recently become achievable thanks to the development of the Brillouin ultraviolet light scattering technique (BUVS) [13–15]. Indeed with this technique it has been possible to investigate in detail the attenuation of vitreous silica suggesting that a crossover between two distinct low- and high-frequency regimes occurs in the frequency (or wave vector) dependence of the sound attenuation [14,15].

These two regimes appear to be dominated by dynamical relaxation processes and phonon scattering due to topological disorder, respectively. In this letter we present the experimental determination of the sound attenuation coefficient of the prototypical strong glass v-GeO_2 over a range spanning more than three decades in frequency.

The choice of v-GeO_2 is twofold: first its low sound velocity has allowed to perform a neutron Brillouin scattering experiment on this sample. The neutrons spectrometry has the advantage of a Gaussian-like shape resolution function, which reflects in a smaller tail of the elastic line when compared to the Lorentzian-like central peaks of a typical inelastic X-rays scattering spectrum in a glass. This allows for a clear detection of the inelastic features of the spectra, and may help in solving the long-lasting debate about the high-frequency dynamics in strong network-forming glasses.

A second reason for studying v-GeO_2 is to clarify whether the above-mentioned crossover can be thought to be a general feature of network-forming glasses, which is related to the existence of dynamical heterogeneities [16–18] as already found in v-SiO_2 [15].

Experiment. – The attenuation coefficients are derived from the energy width Γ at constant q of the Brillouin doublet of the dynamic structure factors measured using three different experimental techniques (BNS from 1 to 5 THz, BLS and BUVS, from 15 to 50 GHz) as well as of those obtained by Molecular Dynamics simulations. We recall that the sound velocity of v-GeO_2[1] is nearly one half that of v-SiO_2, allowing in this case a meaningful BNS investigation [19].

The inelastic neutron scattering data have been obtained using the IN1 and IN8 spectrometers at the Institute Laue Langevin (ILL) in Grenoble (France). In order to gain access to the small q region the configuration of both spectrometers was optimized to operate at low scattering angles (down to 1°). The intensity scattered by the sample was measured in the range of $q = 0.3$–$1.2\,\text{Å}^{-1}$ with 2.5 meV (IN1) and 4.1 meV (IN8) FWHM Gaussian resolution [19]. Corresponding background measurements were collected in the same conditions as the sample. Sample transmission (0.7), background subtraction and multiple scattering were taken into account as in previous experiments [20].

The new high-resolution high-contrast ultraviolet (HIRESUV) spectrometer has been employed for the BUVS measurements. The instrument is based on a home-made 4 m focal length double-grating monochromator specifically designed for Brillouin spectroscopy with ultraviolet (266 nm) excitation [21]. Measurements have been performed at 174° in quasi backscattering configuration with a half-angular aperture of 1.5°. Intrumental intrinsic resolution is about 1 GHz FWHM while the finite aperture instrumental broadening yields a $\frac{\Delta\nu}{\nu}$ of about 1.4×10^{-3}.

The BLS experiments have been performed in 90° and 180° scattering configuration with 514.5 nm excitation and a Sandercock-type (3+3)-pass tandem Fabry-Perot interferometer, with a finesse of about 100 and a contrast greater than 5×10^{10}. BLS measurements were carried out at a mirror spacing of 15.5 mm with a free spectral range of about 9.7 GHz. The instrumental resolution was evaluated by measuring the apparent line width of the inelastic signal produced by an electro-optic transducer [22] which was found to be consistent with the linewidth of the central (elastic) line. A 1 mm wide slit was employed to reduce the peak broadening due to finite gathering angle in the 90° configuration. The residual broadening was calculated and taken into account while fitting the DHO model function, convolved with the instrumental function, to the experimental points. The apparent line width of the Brillouin peaks in the 90° configuration was always found to be at least 1.5 times that of resolution.

The Molecular Dynamic (MD) simulation was performed using 680 GeO_2 units in a 32 Å size cubic box, yielding a density of $\rho = 3.6\,\text{g}\,\text{cm}^{-3}$. The ions interact via a two-body Van Beest type potential [23,24] with parameters suited for the GeO_2 molecule. After the glassy phase has been stabilized, the zero-temperature limit dynamical neutron-weighted structure factors have been calculated diagonalizing the dynamical matrix in the harmonic approximation [25]. A selection of "Brillouin" spectra obtained with different techniques is shown in fig. 1 together with the best fit to the data. The data analysis has been performed using the same model for the three different experiments (including MD) fitting the data with a damped harmonic oscillator (DHO) [26] function plus a delta function convoluted with the appropriate resolution function. The fitting procedure yields the characteristic frequency Ω and the width of the peaks Γ (FWHM). The latter is proportional to the sound attenuation coefficient.

Results and discussion. – The temperature dependence of the attenuation has been measured using both visible and ultraviolet excitation. The values of the internal friction $Q^{-1} = \Gamma/\hbar\omega$ measured with BUVS in backscattering conditions (and therefore at a frequency determined by the longitudinal sound velocity v_l to be $\nu \simeq v_l q/2\pi \simeq 49$ GHz) are shown in fig. 2 together with those measured using visible excitation in the same scattering geometry (hence at about $\nu \simeq 25$ GHz) both in the present work and in reference [27]. The satisfactory agreement (which extends also to measured sound velocity values) between our data obtained with visible radiation and previously published data indicates that our samples are not dissimilar from those used in previous works.

In the same figure we also report curves worked out for thermally activated relaxation processes (TARP) using a Gaussian distribution, $P(V)$, of barriers V having a

[1] All experiments have been performed on home-made glass samples obtained melting a GeO_2 powder (99.99% purity from Aldrich) in an alumina crucible subsequently kept for 5 h at 1600°.

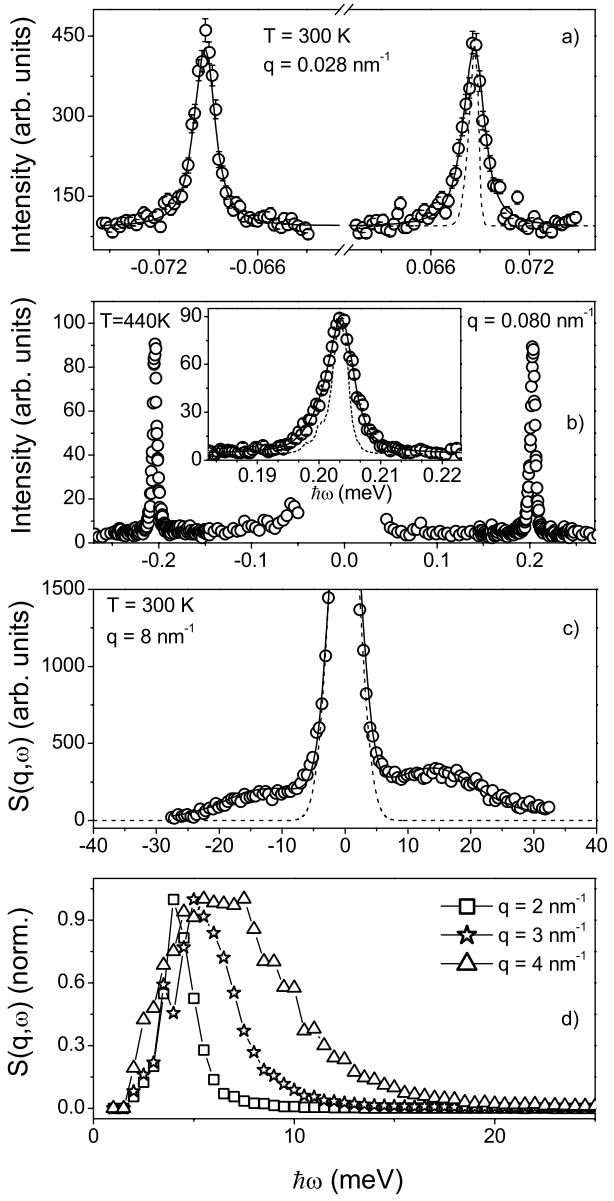

Fig. 1: Selection of spectra from the three experiments and the simulation. a) Brillouin peaks at room temperature obtained with BLS in 90° configuration. b) BUVS spectrum at $T = 440\,\mathrm{K}$ in near backscattering configuration. In the inset the Stokes line is shown. c) BNS spectrum at room temperature. Continuous lines: best fit to the data. Dashed lines: instrumental resolution. d) Dynamic structure factor from the numerical simulation at three different exchanged wave vectors.

variance σ_V [27–29]. For such a model system, assuming that the relaxation is a thermally activated process with a characteristic time $\tau(T) = \tau_0 \exp(V/T)$, one obtains an internal friction [27]:

$$Q_{Th}^{-1}(T,\omega) = \frac{\Gamma^{Th}}{\hbar\omega} = A\int_0^\infty \frac{\omega\tau(T)}{1+\omega^2\tau^2(T)} P(V)\,\mathrm{d}V, \quad (1)$$

where "Th" is for "thermal" and A is a normalizing factor. The figure shows that, if the parameters A and

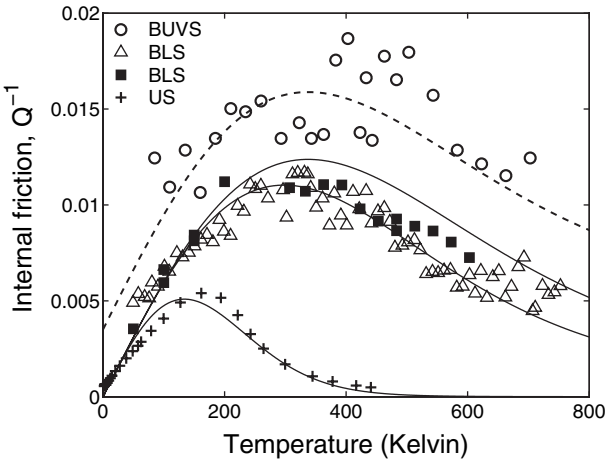

Fig. 2: Temperature dependence of the internal-friction coefficient $Q^{-1} = \Gamma/\hbar\omega$. Circles: BUVS, $q = 0.08\,\mathrm{nm}^{-1}$, present work; triangles: BLS, $q = 0.042\,\mathrm{nm}^{-1}$, from ref. [27]; squares: BLS, $q = 0.0394\,\mathrm{nm}^{-1}$, present work; crosses: US, $\nu \sim 20\,\mathrm{MHz}$, from ref. [2]. The error bars are comparable with the scatter in the data. The continuous curves are computed from equation (1) with parameters: $\sigma_V = 1750\,\mathrm{K}$, $\tau_0 = 1.47 \cdot 10^{-14}\,\mathrm{sec}$ and $A = 0.18$ at three different frequencies (from top to bottom): 49 GHz, 25 GHz and 20 MHz. The disagreement between the upper continuous curve and the BUVS data is systematic and outside the error bars affecting the data. The dashed line is obtained adding to the upper continuous curve the term of eq. (2) with a crossover wave vector $q_c = 0.1\,\mathrm{nm}^{-1}$ and $D \simeq 27 \cdot 10^{-2}\,\mathrm{meV} \cdot \mathrm{nm}^2$, parameters obtained by a simultaneous fit of all the data to eq. (3). The upper continuous and the dashed lines thus both correspond to the same frequency (49 GHz) of the BUVS data.

σ_V are determined fitting the BLS ($\nu \sim 25\,\mathrm{GHz}$) data, a good agreement has been reported with lower frequency ultrasonic attenuation data [27], as shown in fig. 2 for the frequency $\nu \sim 20$ MHz [2]; on the contrary, the model systematically underestimates our experimental findings at the frequency ($\nu \sim 49\,\mathrm{GHz}$) explored by ultraviolet scattering[2].

Concerning the model dependence of our analysis, it should be remarked that the frequency dependence of the model is found to be almost unaffected by the choice of the distribution function as already reported by Gilroy and Phillips [30] in the case of silica. Therefore, it seems that at higher frequency the proposed model becomes inadequate in accounting for the observed sound attenuation. At even higher frequencies (above 1 THz), such as those probed in our BNS experiments, the inadequacy of this model is by far more evident. Our data (see fig. 3) indicate that in this frequency range, at room temperature,

[2]In principle, the presence of photons absorption in the sample gives rise to an additional broadening of the Brillouin peak because of the ill-definition of the wave vector q. At the wavelength used in BUVS experiment, this contribution to the width of the Brillouin peaks can be estimated to be $\Delta\Gamma \sim 2 \cdot 10^{-5}\,\mathrm{meV}$ at $T = 300\,\mathrm{K}$. This value corresponds to an internal friction of $Q^{-1} \sim 1 \cdot 10^{-4}$, negligible with respect to the natural one ($Q^{-1} \sim 0.015$).

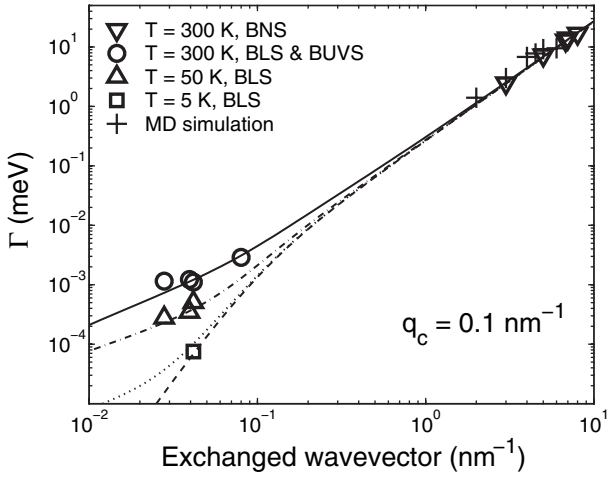

Fig. 3: Γ (full width at half maximum) as a function of the exchanged wave vector q. Down triangles: BNS at room temperature, present work; circles: BUVS and BLS at room temperature, present work and ref. [27]; up triangles: BLS at 50 K, present work; square: BLS at 5 K [31]; crosses: numerical simulation, present work. The curves are computed by means of eq. (3) with the same parameters as in fig. 2 at different temperatures: 300 K (continuous), 50 K (dash-dotted), 5 K (dotted), 0 K (dashed).

$\Gamma \sim Dq^2$ with $D \simeq 27 \cdot 10^{-2}\,\mathrm{meV \cdot nm^2}$, while the model would predict $\Gamma/q^2 \simeq 1.5 \cdot 10^{-2}\,\mathrm{meV \cdot nm^2}$. This suggests that an additional contribution, besides the one due to thermal activated processes, must be included in order to account for Γ at all q values. This contribution appears to behave as q^2 above 1 THz, as already found in several disordered systems [6] including v-SiO_2. In most cases the coefficient D has been found to be temperature independent; even if no experimental proof is available for the case under study, it is worthwhile noticing that the MD results obtained for v-GeO_2 at 0 K yield essentially the same linewidths found by BNS at room temperature. A plausible physical origin for this linewidth contribution has already been suggested for the case of v-SiO_2 as arising from elastic scattering of sound waves from inhomogeneities when the wave vector exceeds some crossover value q_c [15]. The simplest ansatz for such a contribution to the linewidth could therefore be written as

$$\Gamma^{Sc} \sim \frac{Dq^2}{1+(q_c/q)^2}, \tag{2}$$

where "Sc" stands for "elastic scattering". The value of D is determined unambiguously by the BNS results. The wave vector dependence of Γ at different temperatures, as reported in fig. 3, indicates that q_c must lie between the BLS ($q = 0.042\,\mathrm{nm^{-1}}$) data and the lowest q BNS ($q = 3\,\mathrm{nm^{-1}}$) point. An estimate of the q_c value can be deduced from the temperature dependence of the internal friction shown in fig. 2. A simultaneous fit of the BUVS, BLS and US data to

$$Q^{-1} = Q_{Th}^{-1}(T,q) + Q_{Sc}^{-1}(q) \tag{3}$$

gives $q_c = 0.1 \pm 0.05\,\mathrm{nm^{-1}}$.

The resulting temperature dependence of Q^{-1} well fits the UV data (fig. 2, dashed line) explaining the attenuation excess found at this frequency. The value $q_c = 0.1\,\mathrm{nm^{-1}}$ allows to reconstruct the wave vector dependence of Γ at all the measured temperatures as shown in fig. 3. The resulting "static" term, Γ^{Sc}, contributes to the total attenuation, at room temperature, by about 30% around 49 GHz which reduces to a few percent at 25 GHz becoming negligible at ultrasonic frequencies. Such a choice for q_c is in good agreement with the attenuation measured at low temperature at 5 K [31], where Γ^{Th} is vanishingly small[3]. It shall be mentioned that an other attenuation mechanism, the interaction of the sound wave with the thermal vibrations, has been reported in other glasses, such as v-SiO_2 [33] and v-Si [34], to be not negligible in the frequency range where the crossover wave vector q_c is observed. This mechanism gives rise to a plateau in the temperature dependence of the attenuation at high temperatures where the anharmonic effects are more pronounced. The relevance of phonon anharmonicity in determining the attenuation of sound can be evaluated using the high-temperature limit formula for crystals in the dominant phonon approximation namely [3,35,36]

$$\lim_{T\to\infty} Q_l^{-1} = \frac{TCG^2}{\rho_m v_l^2}\omega\tau_{th}, \tag{4}$$

where T, C, G, ρ_m, ω and τ_{th} are the temperature, the heat capacity of the thermal-phonon mode, the Grüneisen parameter, the mass density, the frequency of the sound waves and the phonon population relaxation time, respectively. τ_{th} can be obtained from the thermal conductivity formula $\lambda = \frac{1}{3}C\overline{v}^2\tau_{th}$, where $\overline{v}^2$ is some average phonon velocity which for our purposes can be assumed to be proportional to v_l^2. We can thus compare the relevance of the damping due to anharmonicity between v-GeO_2 and v-SiO_2 assuming, for a given temperature and frequency

$$\lim_{T\to\infty} Q_l^{-1} \propto \frac{G^2\lambda}{\rho_m v_l^4}. \tag{5}$$

While the thermal conductivity λ is very similar for the two substances [37], the other quantities involved differ substantially being for v-SiO_2: $v_l = 5975\,\mathrm{m/s}$, $\rho_m = 2.20\,\mathrm{g/cm^3}$ while for v-GeO_2: $v_l = 3770\,\mathrm{m/s}$, $\rho_m = 3.66\,\mathrm{g/cm^3}$. As far as the values of G^2 are concerned, these have been evaluated assuming that, at the investigated temperatures, the best estimate for the Grüneisen parameter squared, G^2 is the weighted average of

[3] However, it must be taken into account that this compatibility is dependent on the particular ansatz for Γ^{Sc} and that a small contribution from Two Level Systems [29,32] may also be present at such temperatures.

the longitudinal and transverse long-wavelenght mode parameters γ_l^2 and γ_t^2 squared [38], namely

$$G^2 \simeq \frac{1}{3}\left(\gamma_l^2 + 2\gamma_t^2\right). \tag{6}$$

The values of the longitudinal mode γ_l parameter can than be calculated rather consistently for the two substances using available velocity pressure derivatives data [39,40] being [41,42]

$$\gamma_l = \frac{1}{3} + B_T\left(\frac{\partial \log v_l}{\partial P}\right)_T \simeq \frac{1}{3} + \rho_m\left(v_l^2 - \frac{4}{3}v_t^2\right)\left(\frac{\partial \log v_l}{\partial P}\right)_T. \tag{7}$$

We obtain, at room temperature and zero pressure, $\gamma_l = -2.57$ for v-SiO_2, in fair agreement with independent determinations [42,43], and $\gamma_l = -0.06$ for v-GeO_2. Lacking a direct determination of γ_t for v-GeO_2 we will further assume $\gamma_t^2 \simeq \gamma_l^2$ since for v-SiO_2 [42] this assumption is well verified.

With these values one obtains $G^2 = 6.6$ for v-SiO_2 and a much smaller value $G^2 = 0.0036$ for v-GeO_2. Such a large difference in G^2 can be confirmed also revisiting another determination of the mode parameters for v-GeO_2 [44] which however appears to have missed the $\frac{1}{3}$ term in their derivation (we obtain in this case a factor ~ 15 at room temperature). On the basis of these considerations, we have neglected the anharmonic contribution in the present analysis. Furthermore, the absence of a plateau in the case of v-GeO_2 and the good agreement between the TARP model of eq. (1) and the BLS data of fig. 2, seem to confirm our assumption.

The nature of the change in slope of Γ^{Sc}, described by eq. (2) can be interpreted as the effect of heterogeneities of a size, $\xi \sim 2\pi/q_c$, of the order of tens of nanometers. Vibrational heterogeneities are a purely harmonic effect arising from the elastic constant inhomogeneity which seems to be typical of glasses as recently discussed in numerical studies of Lennard-Jones networks and of silica glass [16–18]. They are supposed to mark the transition from an elastic-continuum-like behavior to the atomic-scale dynamics. In particular, when the wavelength of the elastic wave is bigger than ξ, a $\Gamma^{Sc} \sim q^4$ is predicted if the heterogeneities are considered as local impurities [8,45]. A q^4 dependence has been also exploited to explain the plateau of thermal conductivity [46–48]. For wavelengths smaller than ξ the sound attenuation cannot be considered as induced by local impurities any more and a $\Gamma^{Sc} \sim q^2$ is again observed. A possible explanation for the crossover from q^4 to q^2 regime can be found in a recently proposed elastic continuum model [49]. In this framework the crossover in the acoustic attenuation is associated to the onset of the excess in the density of states with respect to the Debye prediction [50,51].

Conclusions. – In the present letter new Brillouin scattering measurements on the prototypical strong glass vitreous germania have been reported. A quantitative evaluation of the anharmonic contribution to the acoustic attenuation indicate that the lowest investigated frequencies are dominated by contributions of dynamical nature. At higher frequencies a crossover point where the static, harmonic contribution overcomes the dynamical terms has been observed, supporting the interpretation that the sound attenuation at the nanometer length scale is induced by the presence of dynamical heterogeneities.

* * *

This work was partially supported by Progetto di Ricerca di Interesse Nazionale "Vibrational dynamics and relaxation phenomena in disordered systems" number 2005023051 funded by MIUR.

REFERENCES

[1] Fontana A., Verrocchio P. and Viliani G. (Editors), *Philos. Mag.*, Special Issue *10th International Workshop on Disordered Systems, Trento, Italy, 18-21 March 2006*, **87** (2007).
[2] Hunklinger S. and Schickfus M. v., *Amorphous Solids, Low Temperature Properties*, edited by Phillips W. A., Vol. **24** (Springer-Verlag, Berlin) 1981, pp. 81-105.
[3] Pine A. S., *Phys. Rev.*, **185** (1969) 1187 and references therein.
[4] Vacher R. and Pelous J., *Phys. Rev. B*, **14** (1976) 823.
[5] Dietsche W. and Kinder H., *Phys. Rev. Lett.*, **43** (1979) 1413; Zhu T. C. *et al.*, *Phys. Rev. B*, **44** (1991) 4281.
[6] Sette F. *et al.*, *Science*, **280** (1998) 1550; Ruffle B. *et al.*, *Phys. Rev. Lett.*, **90** (2003) 095502; Matic A. *et al.*, *Phys. Rev. Lett.*, **93** (2004) 145502; Ruocco G. *et al.*, *Phys. Rev. Lett.*, **83** (1999) 5583.
[7] Grigera T. S. *et al.*, *Phys. Rev. Lett.*, **87** (2001) 085502; Taraskin S. N. and Elliott S. R., *J. Phys.: Condens. Matter*, **14** (2002) 3143; Gotze W. and Mayr M. R., *Phys. Rev. E*, **61** (2000) 587; Dell'Anna R. *et al.*, *Phys. Rev. Lett.*, **80** (1998) 1236; Schirmacher W. *et al.*, *Phys. Rev. Lett.*, **81** (1998) 136; Angelani L. *et al.*, *Phys. Rev. Lett.*, **84** (2000) 4874; Taraskin S. N. and Elliott S. R., *Phys. Rev. B*, **61** (2000) 12017; Verrocchio P., *J. Non-Cryst. Solids*, **352** (2006) 4536.
[8] Buchenau U. *et al.*, *Phys. Rev. B*, **46** (1992) 2798.
[9] Caponi S., Carini G., D'Angelo G., Fontana A., Pilla O., Rossi F., Terki F., Tripodo G. and Woignier T., *Phys. Rev. B*, **70** (2004) 214204.
[10] Hunklinger S. and Arnold W., *Physical Acoustics*, edited by Mason W. P., Vol. **12** (Academic Press) 1976, pp. 155-215.
[11] Angell C. A., *Science*, **267** (1995) 1924.
[12] Price D. L. *et al.*, *Phys. Rev. Lett.*, **81** (1998) 3207.
[13] Masciovecchio C. *et al.*, *Phys. Rev. Lett.*, **92** (2004) 247401; 255507; Baldi G. *et al.*, *J. Non-Cryst. Solids*, **351** (2005) 1919.
[14] Benassi P. *et al.*, *Phys. Rev. B*, **71** (2005) 172201.
[15] Masciovecchio C. *et al.*, *Phys. Rev. Lett.*, **97** (2006) 035501.
[16] Tanguy A. *et al.*, *Phys. Rev. B*, **66** (2002) 174205; Leonforte *et al.*, Cond-mat/0505610 (2005).
[17] Rossi B. *et al.*, *Europhys. Lett.*, **71** (2005) 256.

[18] Leonforte F., Tanguy A., Wittmer J. P. and Barrat J. L., *Phys. Rev. Lett.*, **97** (2006) 055501.
[19] Bove L. E. *et al.*, *Europhys. Lett.*, **71** (2005) 563.
[20] Petrillo C. *et al.*, *Phys. Rev. E*, **62** (2000) 3611.
[21] Benassi P. *et al.*, *Rev. Sci. Instrum.*, **76** (2005) 013904.
[22] Caponi S., Dionigi M., Fioretto D., Mattarelli M., Palmieri L. and Socino G., *Rev. Sci. Instrum.*, **72** (2001) 198.
[23] Taraskin S. N. and Elliott S. R., *Phys. Rev. B*, **56** (1997) 8605.
[24] Taraskin S. N., Loh Y. L., Natarajan G. and Elliott S. R., *Phys. Rev. Lett.*, **86** (2001) 1255.
[25] Pilla O. *et al.*, *J. Phys.: Condens. Matter*, **16** (2004) 8519.
[26] Boon J. P. and Yip S., *Molecular Hydrodynamics* (Dover Publications, Inc., New York) 1980.
[27] Hertling J. *et al.*, *J. Non-Cryst. Solids*, **226** (1998) 129.
[28] Sakai K. *et al.*, *J. Non-Cryst. Solids*, **109** (1989) 47.
[29] Rau S. *et al.*, *Phys. Rev. B*, **52** (1995) 7179.
[30] Gilroy K. S. and Phillips W. A., *Philos. Mag. B*, **43** (1981) 735.
[31] Ruffl\'e B. *et al.*, private communication.
[32] Laermans C. *et al.*, *Phys. Rev. B*, **55** (1997) 2701.
[33] Vacher R. *et al.*, *Phys. Rev. B*, **72** (2005) 214205.
[34] Fabian J. and Allen P. B., *Phys. Rev. Lett.*, **82** (1999) 1478.
[35] Bömmel H. E. and Dransfeld K., *Phys. Rev.*, **117** (1960) 1245.
[36] Woodruff T. O. and Ehrenreich H., *Phys. Rev.*, **123** (1961) 1553.
[37] Zeller R. C. and Pohl R. O., *Phys. Rev. B*, **4** (1971) 2029.
[38] A full theoretical and experimental justification of our assumption is reported in a forthcoming paper, Nardone M. *et al.*, in preparation.
[39] Tielbürger D., Merz R., Ehrenfels R. and Hunklinger S., *Phys. Rev. B*, **45** (1992) 2750.
[40] Hertling J., Baeßler S., Rau S., Kasper G. and Hunklinger S., *J. Non-Cryst. Solids*, **226** (1998) 129.
[41] Phillips W. A., *Amorphous Solids, Low Temperature Properties*, edited by Phillips W. A., Vol. **24** (Springer-Verlag, Berlin) 1981, p. 53.
[42] Wang R. J., Wang W. H., Li F. Y., Wang L. M., Zhang Y., Wen P. and Wang J. F., *J. Phys.: Condens. Matter*, **15** (2003) 603.
[43] Anderson O. L., *Geophys. J. Int.*, **143** (2000) 279.
[44] Soga N., *J. Appl. Phys.*, **40** (1969) 3382.
[45] Klemens P. G., *Proc. Phys. Soc., London*, **68A** (1955) 1113; Parshin D. A., *Phys. Solid State*, **36** (1994) 991.
[46] Raychaudhuri Arup K., *Phys. Rev. B*, **39** (1989) 1927.
[47] Grace J. M. and Anderson A. C., *Phys. Rev. B*, **33** (1986) 7186.
[48] Graebner J. E., Golding B. and Allen L. C., *Phys. Rev. B*, **34** (1986) 5696.
[49] Schirmacher W., *Europhys. Lett.*, **73** (2006) 892.
[50] Schirmacher W., Ruocco G. and Scopigno T., *Phys. Rev. Lett.*, **98** (2007) 079604.
[51] Bove L. E., Petrillo C., Fontana A. and Sokolov A., in preparation.